Journal of Medicinal Chemistry

ARTICLE

pubs.acs.org/jmc

Discovery of Novel and Potent Orally Active Calcium-Sensing Receptor Antagonists that Stimulate Pulselike Parathyroid Hormone Secretion: Synthesis and Structure−Activity Relationships of Tetrahydropyrazolopyrimidine Derivatives†

Masato Yoshida,* Akira Mori, Etsuo Kotani, Masahiro Oka, Haruhiko Makino, Hisashi Fujita, Junko Ban, Yukihiro Ikeda, Tomohiro Kawamoto, Mika Goto, Hiroyuki Kimura, Atsuo Baba, and Tsuneo Yasuma

Pharmaceutical Research Division, Takeda Pharmaceutical Company Limited, 17-85 Jusohonmachi-2-chome, Yodogawa-ku, Osaka 532-8686, Japan

Supporting Information

ABSTRACT: As part of our research for novel calcium-sensing receptor (CaSR) antagonists that can function as oral bone anabolic agents, we recently reported the discovery of a tetrahydropyrazolopyrimidine derivative featuring adamantyl group **1b** with potent CaSR antagonistic activity. To explore the potential of this calcilytic congener, we introduced the *gem*-dialkyl benzyl group at the 3-position of the tetrahydropyrazolopyrimidine ring, forming a bioisostere of the adamantyl group by mimicking the adamantyl group's lipophilicity and bulkiness. Optimization directed toward the improvement of solubility and metabolic stability led to the discovery of compound **9e**, which stimulated transient PTH secretion when orally administered to normal rats. Further, compound **9e** proved to be fully effective in an osteopenic ovariectomized rat model.

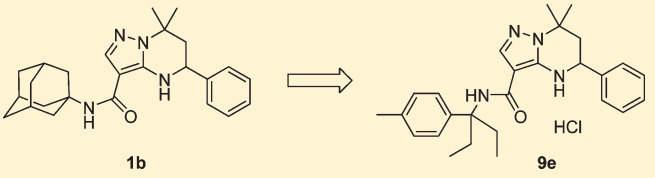

INTRODUCTION

Osteoporosis is characterized by a decrease in bone density, resulting in fragile bones.[1] This disorder of the skeleton weakens bones and increases the risk for fractures. In the United States, direct health care costs from osteoporotic fractures amount to billions of dollars.[2,3] The pathogenesis of osteoporosis involves an imbalanced turnover and a net increase in bone resorption, leading to reduced bone mass and increased risk for fractures. Currently available therapies for osteoporosis include the inhibition of bone resorption through the use of antiresorptive agents (bisphosphonates,[4,5] estradiol, calcitonin, raloxifene,[6] etc.) and promotion of bone formation with anabolic agents[7−9] (recombinant full-length human parathyroid hormone (PTH) 1−84 (Nycomed), and teriparatide, the recombinant N-terminal PTH 1−34 amino acid fragment (Lilly).

PTH is an 84-amino acid peptide, produced by the parathyroid glands, that regulates calcium homeostasis through actions on the kidney and bone. Bone-forming effects and increased bone strength following transient exposure to PTH through intermittent, subcutaneous administration of PTH 1−84 or PTH 1−34 have been well documented in animal models and in healthy human volunteers, as well as in patients with osteoporosis. However, it has become clear that elevated levels of PTH only result in higher bone mass if the increases are transient; continuous infusion of PTH leads to increased bone turnover without net formation, resulting in overall bone loss.[10−12]

The secretion of PTH by parathyroid glands is closely regulated by the calcium-sensing receptor (CaSR),[13] a G-protein coupled receptor (GPCR) highly expressed on parathyroid cells. CaSR detects and responds to small changes in circulating $[Ca^{2+}]$ at the surface of parathyroid cells, leading to regulation of PTH. The receptor is negatively coupled with PTH secretion, such that increasing the concentration of the extracellular ligand $[Ca^{2+}]$ inhibits PTH secretion. It has been proposed that an antagonist of CaSR (calcilytic)[14−17] can mimic hypocalcemia and stimulate PTH secretion.[15]

Targeting this regulatory mechanism by the antagonism of CaSR, leading to the transient and rapid secretion of endogeneous PTH, should promote the formation of new bone analogously to the results found for parenterally administered PTH.[7−9] Therefore, we attempted to identify short-acting CaSR antagonists, and we recently reported the discovery of a tetrahydropyrazolopyrimidine derivative featuring an adamantyl group **1b** with potent CaSR antagonistic activity.[18] However, after the CaSR antagonist was orally administered to normal rats, compound **1b** did not lead to significant PTH secretion, a finding that is consistent with its poor pharmacokinetic (PK) profile. Therefore, we continued to explore the potential of such calcilytic congeners.

To modify compound **1**, a diverse amide library was prepared by high throughput organic synthesis (HTOS), and 4-trifluoromethyl benzyl amide **2a** (IC_{50} = 2900 nM) and benzhydryl amide **2b** (IC_{50} = 380 nM) showed moderate activity. Therefore, we postulated that the bulkiness and lipophilicity of the adamantyl

Received: November 11, 2010
Published: February 09, 2011

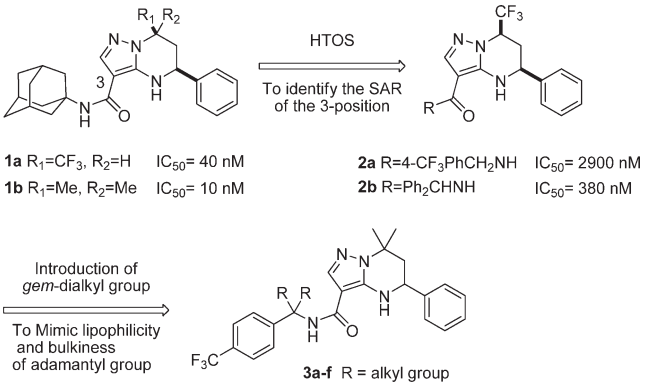

Compound	R	IC_{50} (nM)[a]
3a	Me	3.5 (1.9–6.3)
3b	Et	7.6 (5.0–12)
3c	*n*Pr	4.4 (3.0–6.4)
3d	*n*Bu	23 (15–36)
3e	*i*Pr	30 (20–46)
3f	*c*hex	150 (81–266)

[a] 95% Confidence intervals are shown in parentheses.

Figure 1. Introduction of *gem*-dialkyl benzyl amide on the 3-position.

group are important for maintaining potent activity and introduced the *gem*-dialkyl benzyl amide on the 3-position of the tetrahydropyrazolopyrimidine ring as a bioisostere of the adamantyl group (Figure 1). As a result of this modification, we discovered compounds **3a**−**c**, which showed more potent antagonistic activity than compound **1b**. Compound **3b** showed favorable oral bioavailability (24.4%) in normal rats and stimulated significant increases in PTH concentrations, but it stimulated a sustained PTH pattern and the PK behavior was not desirable for this program.

For endogenous transient PTH secretion by oral administration of a CaSR antagonist, we assumed that a CaSR antagonist should possess high solubility and moderate microsome stability as desirable characteristics because high solubility accelerates absorption and rapid metabolism results in high clearance and a pulse-like PK profile. In this report, we describe the discovery of a short-acting CaSR antagonist and its bone-forming effect in animal osteoporosis models.

CHEMISTRY

The synthesis of 7,7-dimethyl tetrahydropyrazolopyrimidine derivatives **3a**−**f** and **8a**−**j** is shown in Scheme 1. Ethyl 5-amino-1*H*-pyrazole-4-carboxylate **4** was treated with 3-methyl-1-phenylbut-2-en-1-one to afford dihydropyrazolopyrimidine **5**. Reduction of the pyrimidine ring with $NaBH_4$ afforded tetrahydropyrazolopyrimidine **6**, and subsequent hydrolysis with potassium hydroxide (KOH) gave carboxylic acid **7**. Finally, condensation reactions were performed using 2-(1*H*-7-azabenzotriazole-1-yl)-1,1,3,3-tetramethyl uronium hexafluorophosphate (HATU) as a coupling reagent to provide amide derivatives **3a**−**f** and **8a**−**j**. Among them, the 4-chloro analogue **8b** and 4-methyl analogue **8g** were converted to the corresponding salts **9a**−**f** with various acids.

Furthermore, some ester analogues were prepared as shown in Schemes 2 and 3. In the case of benzoate **10**, the ester group was introduced to the iodo analogue **8i** using 1,1′-bis(diphenylphosphino)ferrocene (dppf) and palladium(II) acetate under a carbon monoxide atmosphere. Ethyl ester **10** was reduced to benzyl alcohol **11** using lithium aluminum hydride, and successive treatment with acetyl chloride in the presence of potassium carbonate (K_2CO_3) afforded acetate **12**. Phenyl ester analogue **14a** was synthesized by acylation of phenol **13**, which was prepared from **8j** by removal of the benzyl group, using 10% Pd−C under a hydrogen atmosphere. Phenoxyacetate **14b** was also prepared from phenol **13** by alkylation, using ethyl bromoacetate in the presence of K_2CO_3.

Among the compounds prepared, compound **9e** stimulated pulse-like PTH secretion in rats, and therefore, enantiomers of **9e** were prepared, as shown in Scheme 4. Racemic ester **6** was separated by preparative high-performance liquid chromatography (HPLC) using a chiral column [CHIRALPAK OD, hexane/ethanol = 95:5] to afford both enantiomers, **15a** and **15b** with high enantiomeric purity (>99% ee). Enantiomers **15a** and **15b** were then converted to amide derivatives (−)-**17a** and (+)-**17b**, respectively, by alkaline hydrolysis with KOH and a subsequent coupling reaction with 3-(4-methylphenyl)pentan-3-amine. Their absolute configuration was confirmed by X-ray analysis of 4-trifluoromethyl analogue **17c**,[19] which was derived from ester **15b**. The X-ray crystal structure of **17c** is shown in Figure 2. This result showed that the absolute configurations of (−)-**17a** and (+)-**17b** were (*R*)- and (*S*)-forms, respectively.

RESULTS AND DISCUSSION

The compounds synthesized were evaluated for CaSR antagonistic activity using a GTP-binding assay, for which membrane fractions were prepared from CaSR-expressing CHO cells. The results are summarized in Tables 1 and 3.

To estimate the in vivo PTH secretion stimulated by these compounds, plasma PTH levels were assayed using a rat enzyme-linked immunosorbent assay (ELISA) kit (Rat Bioactive Intact PTH ELISA kit, Immutopics, Inc.) after oral administration of the compounds to rats at a dose of 10 mg/kg. The bone-forming effect of these compounds in osteopenic ovariectomized (OVX) rats was evaluated after they were orally administered daily for 13 weeks.[9] Increases in the plasma level of the bone formation marker osteocalcin and bone mineral density (BMD) of the distal femur were measured.

To develop a short-acting CaSR antagonist, we expected that improving solubility by salt formation and optimizing metabolic stability would impart the necessary characteristics to the CaSR antagonist so that it could stimulate transient PTH secretion. In the structure−activity relationship (SAR) study described in our previous report,[18] introducing a side chain containing an amide linker at the 3-position was effective for conferring antagonistic activity. Therefore, we expanded our SAR study of substituents on the phenyl ring at the 3-position. As shown in Table 1, introduction of a chlorine atom or a fluorine atom at the 2- or 3-position of the phenyl ring (**8c**, **8e**, and **8f**) resulted in slightly decreased antagonistic activity compared with that of 4-halophenyl compounds **8b** and **8d**. Therefore, we focused on the substitution at the 4-position of the phenyl ring, and several groups such as alkyl, alkoxy, and ester were introduced to adjust metabolic stability. The methyl analogue, **8g**, and alkoxy analogues **8h** and **8j** exhibited potent antagonistic activity similar to compound **3b**. In the case of ester analogues, ethyl benzoate **10** was tolerated, but benzyl acetate **12**, phenyl acetate **14a**, and phenyl propanoate **14b** had reduced activities. Substitution at the 4-position of the phenyl ring provided compounds with a diverse

Scheme 1. Synthesis of Tetrahydropyrazolopyrimidine 3, 8, and 9[a]

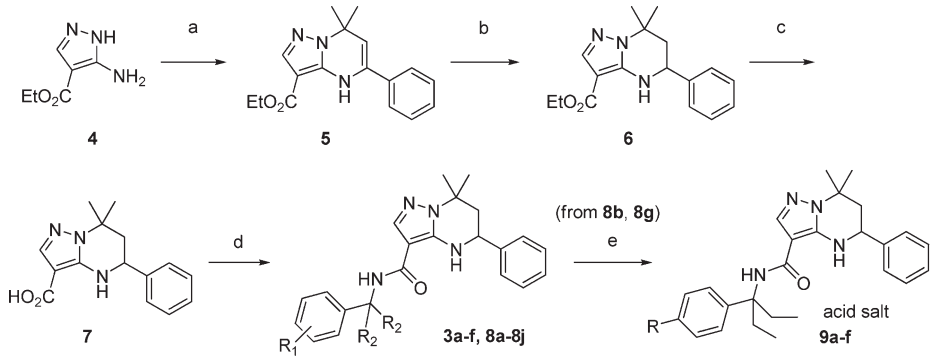

3a : R1=4-CF_3, R2=Me
3b : R1=4-CF_3, R2=Et
3c : R1=4-CF_3, R2=nPr
3d : R1=4-CF_3, R2=nBu
3e : R1=4-CF_3, R2=iPr
3f : R1=4-CF_3, R2=chex

8a : R1=H, R2=Et
8b : R1=4-Cl, R2=Et
8c : R1=3-Cl, R2=Et
8d :R1=4-F, R2=Et
8e : R1=3-F, R2=Et

8f : R1=2-F, R2=Et
8g : R1=4-Me, R2=Et
8h : R1=4-MeO, R2=Et
8i : R1=4-I, R2=Et
8j : R1=4-BnO, R2=Et

9a : R=Cl, Salt : HCl
9b : R=Cl, Salt : $MeSO_3H$
9c : R=Cl, Salt : H_2SO_4
9d : R=Cl, Salt : AcOH
9e : R=Me, Salt : HCl
9f : R=Me, Salt : $MeSO_3H$

[a] Reagents and conditions: (a) $Me_2C{=}CHCOPh$, NaH, DMF; (b) $NaBH_4$, EtOH; (c) KOH, EtOH, H_2O; (d) amine, HATU, iPr_2EtN, DMF; (e) acid.

Scheme 2. Synthesis of Esters 10 and 12[a]

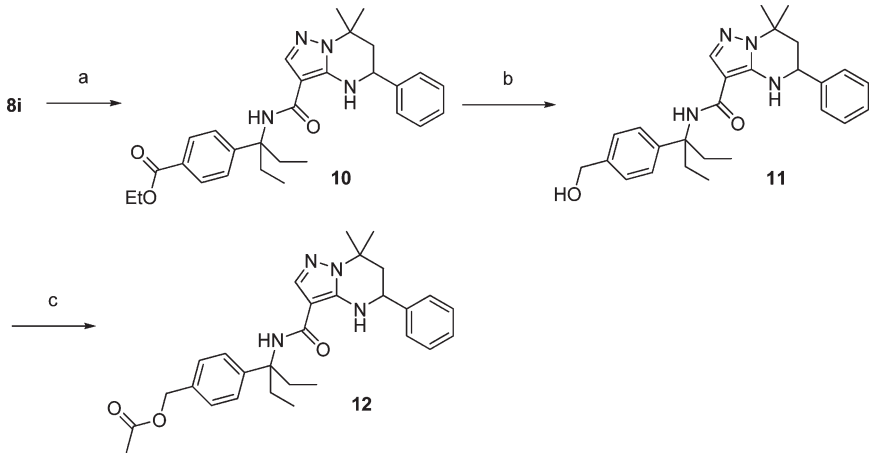

[a] Reagents and conditions: (a) dppf, Pd $(OAc)_2$, Et_3N, CO, EtOH; (b) LAH, THF; (c) AcCl, Et_3N, K_2CO_3, THF.

Scheme 3. Synthesis of Ester 14[a]

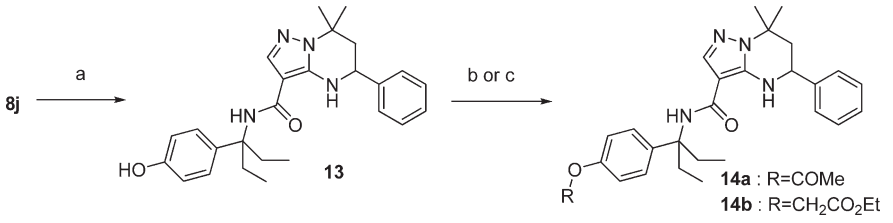

[a] Reagents and conditions: (a) H_2, 10% Pd−C; (b) AcCl, Et_3N, THF; (c) $BrCH_2CO_2Et$, K_2CO_3, DMF.

range of in vitro metabolic stabilities, as shown in Table 1. All the highly potent analogues (**8a**, **8b**, **8d**, **8g**−**j**, and **10**) showed more rapid metabolizing profiles in rat liver microsomes than the lead compound, **3b**.

Next, to confirm the importance of solubility for rapid absorption, we selected compound **8b**, which has high solubility, and prepared salts **9a**−**d** with various acids. The solubility of these salts was measured under a pH 6.8 buffer with bile acid. As shown in Table 2, all the salts (**9a**−**d**) showed increased solubility compared to the free form, **8b**. Compound **8b** and its acetate salt **9d**, which has highest solubility among salts, were tested in an in vivo assay. When **9d** was orally administered, the peak of PTH

dx.doi.org/10.1021/jm101452x |*J. Med. Chem.* 2011, 54, 1430–1440

Scheme 4. Synthesis of Chiral Isomer 17[a]

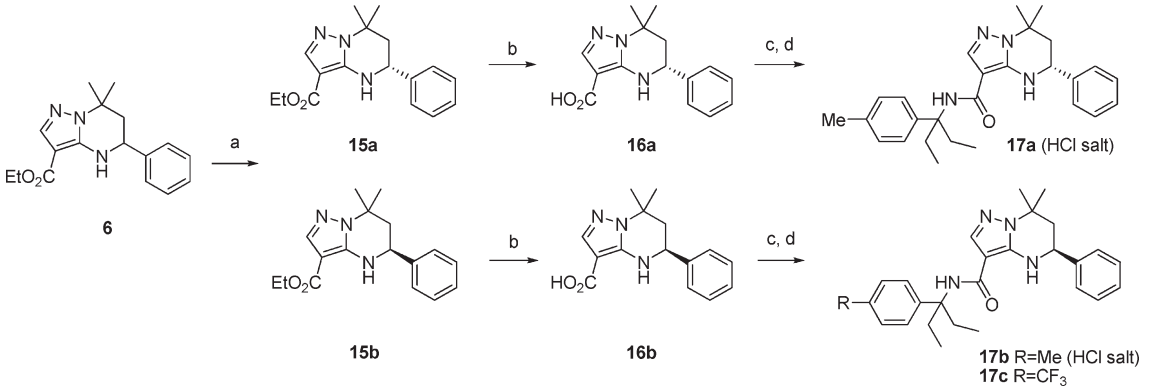

[a] Reagents and condition: (a) CHIRALCEL OD; (b) KOH, EtOH, H_2O; (c) $SOCl_2$, DMF, toluene, then amine, Et_3N, toluene; (d) 4 M HCl in EtOAc.

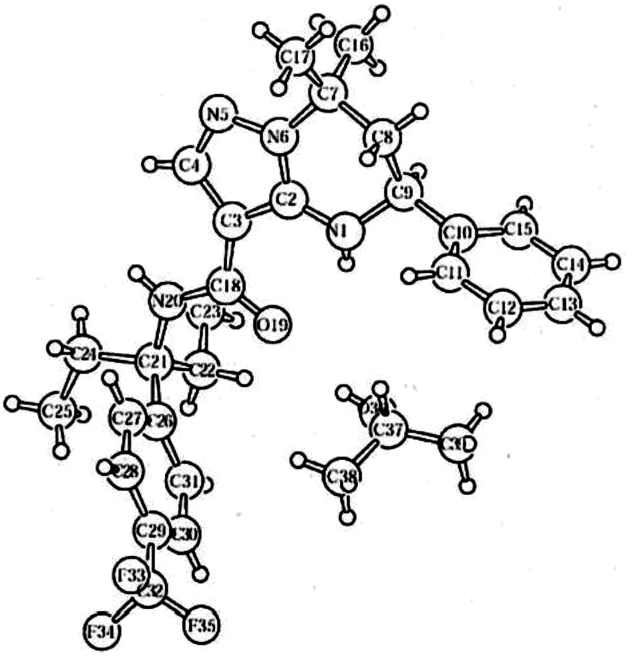

Figure 2. X-ray Crystal Structure of **17c**.

secretion in plasma was higher and earlier than that with the free form, **8b**; however, the plasma PTH secretion pattern was sustained (Figure 3). This result suggests that the rat metabolic stability (57 μL/min/mg) of **9d** is still too high to achieve a transient PTH increase in plasma. Second, we prepared salts of the methyl analogue **8g**, which showed more rapid metabolism (164 μL/min/mg) in rat liver microsomes than compound **8b**. The HCl salt **9e** and MsOH salt **9f** also displayed excellent solubility compared with the free form **8g**. Figure 3 shows the effects of PTH secretion after normal rats were orally administered 10 mg/kg **9e**. The plasma PTH level after oral administration of **9e** increased to 120 pg/mL after 30 min and dropped to normal levels after 2 h. The PK profile of compound **9e** was evaluated after it was orally administered to female SD rats. As shown in Figure 4, compound **9e** displayed good oral absorption and the correlation between the PTH pattern and plasma concentration of compound **9e** was observed. Because the metabolic stability of **9e** in human liver microsomes is similar to that in rat liver microsomes, a transient PTH increase is also expected in humans after oral administration of **9e**.

Membrane permeability (Caco-2) data for **3b**, **8b**, and **9e** are summarized in Table 2. Compounds **3b**, **8b**, and **9e** had almost the same antagonistic activity and membrane permeability. These findings support our speculation that solubility and metabolic stability significantly influence rapid plasma PTH release and decrease, respectively.

We turned our attention to the activities of enantiomers of **9e**, (−)-form **17a** and (+)-form **17b**, in order to investigate the stereochemical requirement for antagonistic activity. As expected, a significant difference in antagonistic activity was observed between the (+) and (−) enantiomers, and (−)-form **17a** (IC_{50} = 2.3 nM) exhibited approximately 10-fold more potent activity than (+)-form **17b** (IC_{50} = 31 nM), as shown in Table 3.

On the basis of the clinical data for teriparatide (PTH 1−34), the PTH pattern achieved with compound **9e** (magnitude and duration) indicated that this compound is effective as a bone anabolic agent for bone formation. Therefore, we tested compound **9e** in OVX rats.[20] In the OVX rat model, female rats experienced accelerated bone loss, similar to the estrogen-deficiency bone loss in postmenopausal women. For 3 months, OVX rats were orally administered 10 mg/kg compound **9e**. Their BMD and plasma osteocalcin (bone metabolic marker) concentration after a 3 month treatment with compound **9e** were compared to those of vehicle control and sham-operated rats (Table 4). Vehicle control OVX rats showed a significant decrease in BMD compared to sham-operated rats, and treatment with compound **9e** significantly increased the BMD of OVX rats. Furthermore, **9e** increased the plasma osteocalcin concentration, consistent with an elevation in bone formation activity. Thus, **9e** proved to be fully effective as a bone anabolic agent in the OVX rat model.

CONCLUSION

An orally active tetrahydropyrazolopyrimidine derivative that stimulated transient PTH secretion has been identified. We found that good solubility and adequate metabolic stability are critical factors for the rapid and transient secretion of PTH. Given the efficacy of compound **9e** in an OVX rat model of bone loss, the magnitude and short action of this compound on plasma PTH levels are expected to stimulate new bone formation even in humans.

Table 1. SAR Summary of Tetrahydropyrazolopyrimidine Analogues as Determined via a GTP-Binding Assay

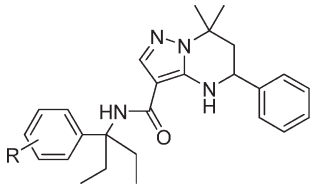

			metabolic stability (μL/min/mg)		
compd	R	CaSR antagonistic activity IC_{50} (nM)[a]	rat	human	solubility (μg/mL)[b]
3b	4-CF_3	7.6 (5.0−12)	13	14	4.6
8a	H	3.4 (1.6−7.1)	215	209	22.3
8b	4-Cl	7.4 (3.7−15)	57	18	54
8c	3-Cl	17 (6.5−44)			
8d	4-F	7.3 (4.6−12)	129	89	8.5
8e	3-F	25 (9.6−63)			
8f	2-F	12 (8.1−16)			
8g	4-Me	5.5 (2.1−14)	164	122	15.6
8h	4-MeO	6.6 (4.2−10)	158	67	59.6
8j	4-BnO	8.5 (3.3−22)	24	48	24.3
10	4-CO_2Et	5.2 (2.4−11)	138[c]	91[c]	5.4
12	4-CH_2OCOMe	14 (7.8−23)			
14a	4-OCOMe	31 (12−83)			
14b	4-OCOEt	12 (5.3−27)			

[a] 95% confidence intervals are shown in parentheses. [b] Buffer (pH6.8)+bile acid. [c] Data of HCl salt.

EXPERIMENTAL SECTION

Chemistry. Melting points were determined on a Yanagimoto micromelting point apparatus or BÜCHI B-545 and uncorrected. ^{1}H NMR spectra of deuteriochloroform ($CDCl_3$) or dimethyl sulfoxide (DMSO-d_6) solution (internal standard tetramethylsilan (TMS), δ 0) were recorded on a Varian Gemini-200, Mercury-300 or Bruker AVANCE-300. Reaction were followed by TLC on Silica Gel 60 F 254 precoated TLC plates (E. Merck) or NH TLC plates (Fuji Silysia Chemical Ltd.). Column chromatography was performed with WAKO Gel 300 using the indicated eluents. We carried out elemental analysis (C, H, N) to determine purity of test compounds by the Analytical Department of Takeda Chemical Industries, and the results were within 0.4% of theoretical values. Purity of compounds (>95%) was established by elemental analysis. The data of elemental analysis is in the Supporting Information.

*Ethyl 7,7-Dimethyl-5-phenyl-4,5,6,7-tetrahydropyrazolo[1,5-a]pyrimidine-3-carboxylate (**6**).* To a solution of **4** (54.3 g, 0.35 mol) in DMF (400 mL) was added sodium hydride (14.0 g, 60% in oil, 0.35 mol) at room temperature. After stirring at the same temperature for 30 min, a solution of 3-methyl-1-phenyl-2-buten-1-one (40.0 g, 0.25 mol) in DMF (20 mL) was added to the reaction mixture. After stirring at room temperature for 2 h, the reaction mixture was quenched with EtOH (400 mL) and stirring for 5 min. After that, $NaBH_4$ (37.8 g, 1.0 mol) was added to the reaction mixture at 0 °C. After stirring at room temperature for 2 h, the solvent was concentrated in vacuo. The residue was diluted with EtOAc and washed with water. The aqueous layer separated was extracted with EtOAc. The organic layer combined was successively washed with 1 M HCl, water and brine, dried over $MgSO_4$, and concentrated in vacuo. The residue was diluted with EtOAc−hexane (1:1, 200 mL), and silicagel (50 g, WAKO Gel 300) was added thereto. After stirring at room temperature for 20 min, inorganic product was filtered off, and the solvent was concentrated in vacuo. Crystallization from EtOAc−hexane afforded **6** (39.2 g, 54%) as white prisms. ^{1}H NMR ($CDCl_3$): δ 1.31 (3H, t, J = 7.0 Hz), 1.57 (3H, s), 1.64 (3H, s), 2.11−2.15 (2H, m), 4.23 (2H, q, J = 7.0 Hz), 4.64 (1H, dd, J = 9.4, 5.2 Hz), 6.03 (1H, s), 7.31−7.45 (5H, m), 7.64 (1H, s).

*7,7-Dimethyl-5-phenyl-4,5,6,7-tetrahydropyrazolo[1,5-a]pyrimidine-3-carboxylic acid (**7**).* A mixture of **6** (13.5 g, 45.1 mmol) and KOH (12.65 g, 225 mmol) in EtOH−H_2O (100 + 100 mL) was stirred at 80 °C for 14 h and concentrated in vacuo. The residue was acidified with citric acid solution and extracted with EtOAc. The extract was washed with water and brine, dried over $MgSO_4$, and then concentrated to afford a solid, which was recrystallized from EtOAc−hexane to give **7** (8.1 g, 66%) as colorless prisms; mp 156−157 °C. ^{1}H NMR ($CDCl_3$): δ 1.57 (3H, s), 1.63 (3H, s), 2.04−2.18 (2H, m), 4.63 (1H, dd, J = 10.2, 5.1 Hz), 5.99 (1H, s), 7.32−7.42 (5H, m), 7.68(1H, s).

*N-(1-Ethyl-1-phenylpropyl)-7,7-dimethyl-5-phenyl-4,5,6,7-tetrahydropyrazolo[1,5-a]-pyrimidine-3-carboxamide (**8a**).* A mixture of **7** (0.50 g, 1.84 mmol), HATU (0.84 g, 2.21 mmol), and iPr$_2$NEt (0.71 g, 5.52 mmol) in DMF (3 mL) was stirred at room temperature for 1 h, followed by an addition of 3-phenylpentan-3-amine hydrochloride (0.44 g, 2.21 mmol). The whole was stirred at 80 °C overnight and concentrated in vacuo. The residue was diluted with EtOAc, washed with aqueous $NaHCO_3$ solution and brine, dried over $MgSO_4$, and concentrated in vacuo. The residue was chromatographed on SiO_2 with EtOAc−hexane (1:1) to give **8a** as crystals (0.36 g, 47%), mp 139−140 °C (EtOAc−hexane). ^{1}H NMR ($CDCl_3$): δ 0.72−0.83 (6H, m), 1.58 (3H, s), 1.66 (3H, s), 1.96−2.26 (6H, m), 4.55 (1H, dd, J = 10.6, 3.2 Hz), 5.63 (1H, s), 6.49 (1H, s), 7.20−7.39 (10H, m), 7.58 (1H, s). Anal. ($C_{26}H_{32}N_4O$) C, H, N.

Table 2. Solubility and Membrane Permeability (Caco-2) Data for 3b, 8b, 8g, and 9a−f

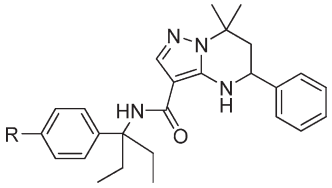

				Caco-2	
compd	R	salt	solubility (μg/mL)[a]	A to B	B to A
3b	CF_3	free	4.6	32.7	24.2
8b	Cl	free	54	52.6	36.8
9a	Cl	HCl	126		
9b	Cl	$MeSO_3H$	164		
9c	Cl	H_2SO_4	202		
9d	Cl	AcOH	202		
8g	Me	free	15.6		
9e	Me	HCl	140	58.9	42.7
9f	Me	$MeSO_3H$	118		

[a] Buffer (pH6.8) + bile acid.

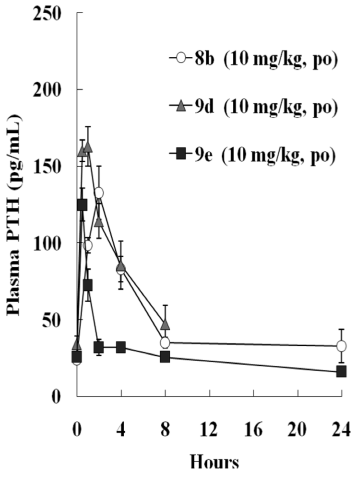

Figure 3. Effects of CaSR Antagonists on PTH Secretion in Normal Rats (n = 4).

The following compounds **3a−f**, **8b−j** were prepared by a manner similar to that used for **8a**.

7,7-Dimethyl-N-{1-methyl-1-[4-(trifluoromethyl)phenyl]ethyl}-5-phenyl-4,5,6,7-tetrahydropyrazolo[1,5-a]pyrimidine-3-carboxamide (***3a***). White prisms (Yield 44%), mp 182−183 °C (EtOAc−hexane). ^{1}H NMR ($CDCl_3$): δ 1.56 (3H, s), 1.64 (3H, s), 1.70 (3H, s), 1.76 (3H, s), 2.02−2.23 (2H, m), 4.54 (1H, dd, J = 11.4, 3.4 Hz), 5.79 (1H, s), 6.42 (1H, s), 7.30−7.31 (5H, m), 7.50 (1H, s), 7.54−7.59 (4 h, s). Anal. ($C_{25}H_{27}F_3N_4O$) C, H, N.

N-{1-Ethyl-1-[4-(trifluoromethyl)phenyl]propyl}-7,7-dimethyl-5-phenyl-4,5,6,7-tetrahydropyrazolo[1,5-a]pyrimidine-3-carboxamide (***3b***). White prisms (yield 60%), mp 188−189 °C (EtOAc−hexane). ^{1}H NMR ($CDCl_3$): δ 0.73−0.89 (6H, m), 1.58 (3H, s), 1.65 (3H, s), 1.89−2.33 (6H, m), 4.54 (1H, dd, J = 11.4, 3.6 Hz), 5.57 (1H, s), 6.41 (1H, m), 7.27−7.58 (10H, s). Anal. ($C_{27}H_{31}F_3N_4O$) C, H, N.

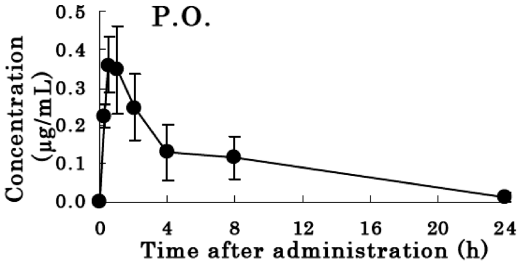

10mg/kg, po	Mean ± S.D. (n=3)
Cmax (μg/mL)	0.374 ± 0.094
Tmax (h)	0.67 ± 0.29
AUC0-24h (μg·h/mL)	2.463 ± 0.71
MRT (h)	5.65 ± 0.86

Figure 4. Pharmacokinetic Parameters for **9e** after Oral Administration in Rat.

Table 3. CaSR Antagonist Activity of 4-Methyl Analogues

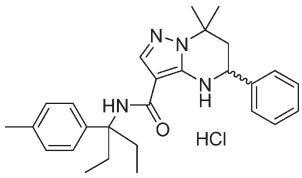

compd	form	IC_{50} (nM)[a]
9e	racemic	4.9 (2.9−8.2)
17a	(−)	2.3 (0.86−6.4)
17b	(+)	31.0 (11−86)

[a] 95% confidence intervals are shown in parentheses.

Table 4. Bone-Forming Effect of Compound 9e in OVX Rat Models

			OVX
	sham	OVX	**9e**
osteocalcin (ng/mL)[a]	16.7 ± 1.1	21.1 ± 2.4	28.4 ± 2.3*[c]
distal femur BMD (mg/cm^3)[b]	737 ± 11	622 ± 7	660 ± 6**[c]
proximal tibia BMD (mg/cm^3)[b]	722 ± 12	649 ± 8	700 ± 5**[c]

[a] After 2 months. [b] Measured by animal CT. [c] *, P < 0.01; **, P < 0.05 vs OVX (Student's t-test).

7,7-Dimethyl-5-phenyl-N-{1-propyl-1-[4-(trifluoromethyl)phenyl]-butyl}-4,5,6,7-tetrahydropyrazolo[1,5-a]pyrimidine-3-carboxamide (***3c***). White prisms (yield 21%), mp 175−176 °C (EtOAc−hexane). ^{1}H NMR ($CDCl_3$): δ 0.85−0.95 (6H, m), 1.00−1.30 (4H, m), 1.57 (3H, s), 1.64 (3H, s), 1.85−2.23 (6H, m), 4.55 (1H, dd, J = 11.0, 3.2 Hz), 5.56 (1H, s), 6.37 (1H, s), 7.28−7.57 (9H, m), 7.49 (1H, s). Anal. ($C_{29}H_{35}F_3N_4O$) C, H, N.

N-{1-Butyl-1-[4-(trifluoromethyl)phenyl]pentyl}-7,7-dimethyl-5-phenyl-4,5,6,7-tetrahydropyrazolo[1,5-a]pyrimidine-3-carboxamide (***3d***). White prisms (yield 10%), mp 113−114 °C (EtOAc−hexane). ^{1}H

dx.doi.org/10.1021/jm101452x |J. Med. Chem. 2011, 54, 1430–1440

NMR ($CDCl_3$): δ 0.82−1.43 (14H, m), 1.59 (3H, s), 1.66 (3H, s), 1.88−2.24 (6H, m), 4.54−4.57 (1H, m), 5.70 (1H, s), 6.44 (1H, s), 7.33−7.64 (10H, m). Anal. ($C_{31}H_{39}F_3N_4O\cdot0.5H_2O$) C, H, N.

*N-{1-Isopropyl-2-methyl-1-[4-(trifluoromethyl)phenyl]propyl}-7,7-dimethyl-5-phenyl-4,5,6,7-tetrahydropyrazolo[1,5-a]pyrimidine-3-carboxamide Hydrochloride (**3e**).* White prisms (yield, 37%), mp 140−142 °C (iPr_2O). ^1H NMR ($CDCl_3$, free form): δ 0.73 (3H, dd, *J* = 6.6, 3.0 Hz), 1.11 (3H, dd, *J* = 6.6, 3.0 Hz), 1.21 (3H, d, *J* = 2.0 Hz), 1.49 (3H, s), 1.57 (3H, s), 1.63 (3H, d, *J* = 2.0 Hz), 2.02−2.40 (3H, m), 3.41 (1H, dd, *J* = 8.8, 2.0 Hz), 4.62 (1H, td, *J* = 11.2, 3.8 Hz), 5.24 (1H, brs), 6.47 (1H, brs), 7.24−7.58 (10H, m). Anal. ($C_{29}H_{36}ClF_3N_4O$) C, H, N.

*N-{Dicyclohexyl[4-(trifluoromethyl)phenyl]methyl}-7,7-dimethyl-5-phenyl-4,5,6,7-tetrahydropyrazolo[1,5-a]pyrimidine-3-carboxamide Hydrochloride (**3f**).* White prisms (yield 20%), mp 146−147 °C (EtOAc−hexane). ^1H NMR ($CDCl_3$): δ 0.71−2.48 (29H, m), 3.40 (1H, brs), 6.47 (1H, brs), 6.95 (1H, brs), 7.43−7.51 (11H, m). Anal. ($C_{35}H_{44}ClF_3N_4O\cdot1.0H_2O$) C, H, N.

*N-[1-(4-Chlorophenyl)-1-ethylpropyl]-7,7-dimethyl-5-phenyl-4,5,6,7-tetrahydropyrazolo-[1,5-a]pyrimidine-3-carboxamide (**8b**).* White prisms (yield, 56%), mp 125−126 °C (Et_2O−hexane). ^1H NMR ($CDCl_3$): δ 0.71−0.85 (6H, m), 1.57 (3H, s), 1.64 (3H, s), 1.85−2.29 (6H, m), 4.54 (1H, dd, *J* = 11.0, 3.4 Hz), 5.52 (1H, s), 6.14 (1H, s), 7.26−7.34 (9H, m), 7.50 (1H, s). Anal. ($C_{26}H_{31}ClN_4O$) C, H, N.

*N-[1-(3-Chlorophenyl)-1-ethylpropyl]-7,7-dimethyl-5-phenyl-4,5,6,7-tetrahydropy-razolo-[1,5-a]pyrimidine-3-carboxamide (**8c**).* White prisms (yield, 65%), mp 195−196 °C (EtOAc−hexane). ^1H NMR ($CDCl_3$): δ 0.72−0.83 (6H, m), 1.58 (3H, s), 1.64 (3H, s), 1.85−2.26 (6H, m), 4.54 (1H, dd, *J* = 11.0, 3.0 Hz), 5.52 (1H, s), 6.40 (1H, s), 7.16−7.38 (9H, m), 7.50 (1H, s). Anal. ($C_{26}H_{31}ClN_4O$) C, H, N.

*N-[1-Ethyl-1-(4-fluorophenyl)propyl]-7,7-dimethyl-5-phenyl-4,5,6,7-tetrahydropy-razolo-[1,5-a]pyrimidine-3-carboxamide (**8d**).* White prisms (yield, 54%), mp 155−156 °C (EtOAc−hexane). ^1H NMR ($CDCl_3$): δ 0.73−0.82 (6H, m), 1.61 (3H, s), 1.70 (3H, s), 1.91−2.30 (6H, m), 4.55 (1H, dd, *J* = 11.4, 3.3 Hz), 5.91 (1H, s), 6.59 (1H, s), 6.96−7.02 (2H, m), 7.29−7.36 (7H, m), 7.87 (1H, s). Anal. ($C_{26}H_{31}FN_4O$) C, H, N.

*N-[1-Ethyl-1-(3-fluorophenyl)propyl]-7,7-dimethyl-5-phenyl-4,5,6,7-tetrahydropy-razolo-[1,5-a]pyrimidine-3-carboxamide (**8e**).* White prisms (yield, 51%), mp 180−181 °C (EtOAc−hexane). ^1H NMR ($CDCl_3$): δ 0.72−0.84 (6H, m), 1.57 (3H, s), 1.64 (3H, s), 1.86−2.30 (6H, m), 4.54 (1H, dd, *J* = 11.0, 3.2 Hz), 5.54 (1H, s), 6.41 (1H, s), 6.84−6.94 (1H, m), 7.03−7.16 (2H, m), 7.28−7.39 (6H, m), 7.51 (1H, s). Anal. ($C_{26}H_{31}FN_4O$) C, H, N.

*N-[1-Ethyl-1-(2-fluorophenyl)propyl]-7,7-dimethyl-5-phenyl-4,5,6,7-tetrahydropy-razolo-[1,5-a]pyrimidine-3-carboxamide (**8f**).* Amorphous solid (yield, 64%). ^1H NMR ($CDCl_3$): δ 0.74−0.83 (6H, m), 1.56 (3H, s), 1.63 (3H, s), 2.01−2.38 (6H, m), 4.54 (1H, dd, *J* = 12.0, 3.3 Hz), 5.65 (1H, s), 6.38 (1H, s), 6.94−7.48 (9H, m), 7.48 (1H, s). Anal. ($C_{26}H_{31}FN_4O$) C, H, N.

*N-[1-Ethyl-1-(4-methylphenyl)propyl]-7,7-dimethyl-5-phenyl-4,5,6,7-tetrahydrop-yrazolo[1,5-a]pyrimidine-3-carboxamide (**8g**).* White prisms (yield, 38%), 155−157 °C (Et_2O−hexane). ^1H NMR ($CDCl_3$): δ 0.72−0.81 (6H, m), 1.59 (3H, s), 1.64 (3H, s), 1.96−2.23 (6H, m), 2.30 (3H, s), 4.54 (1H, dd, *J* = 11.7, 3.3 Hz), 5.55 (1H, s), 6.45 (1H, s), 7.12 (2H, d, *J* = 7.8 Hz), 7.23−7.38 (7H, m), 7.51 81H, s), 7.49 (1H, s). Anal. ($C_{27}H_{34}N_4O\cdot0.1H_2O$) C, H, N.

*N-[1-Ethyl-1-(4-methoxyphenyl)propyl]-7,7-dimethyl-5-phenyl-4,5,6,7-Tetrahydr-opyrazolo[1,5-a]pyrimidine-3-carboxamide (**8h**).* White prisms (yield, 40%), mp 140−141 °C (Et_2O−hexane). ^1H NMR ($CDCl_3$): δ 0.71−0.89 (6H, m), 1.57 (3H, s), 1.64 (3H, s), 1.93−2.27 (6H, m), 3.78 (3H, s), 4.55 (1H, dd, *J* = 11.4, 3.4 Hz), 5.53 (1H, s), 6.45 (1H, s), 6.85 (2H, d, *J* = 8.8 Hz), 7.23−7.40 (7H, m), 7.48 (1H, s). Anal. ($C_{27}H_{34}N_4O_2$) C, H, N.

*N-[1-Ethyl-1-(4-iodophenyl)propyl]-7,7-dimethyl-5-phenyl-4,5,6,7-tetrahydropyrazolo[1,5-a]pyrimidine-3-carboxamide (**8i**).* White prisms (yield, 65%), mp 182−183 °C (Et_2O−hexane). ^1H NMR ($CDCl_3$): δ 0.71−0.83 (6H, m), 1.56 (3H, s), 1.64 (3H, s), 1.84−2.28 (6H, m), 4.54 (1H, dd, *J* = 11.0, 3.4 Hz), 5.50 (1H, s), 6.40 (1H, s), 7.11 (2H, d, *J* = 8.8 Hz), 7.27−7.37 (5H, m), 7.49 (1H, s), 7.61 (2H, d, *J* = 8.8 Hz). Anal. ($C_{26}H_{31}IN_4O$) C, H, N.

*N-{1-[4-(Benzyloxy)phenyl]-1-ethylpropyl}-7,7-dimethyl-5-phenyl-4,5,6,7-tetrahydropyrazolo[1,5-a]pyrimidine-3-carboxamide (**8j**).* White prisms (yield, 83%), mp 130−131 °C (EtOAc−hexane). ^1H NMR ($CDCl_3$): δ 0.73−0.81 (6H, m), 1.56 (3H, s), 1.64 (3H, s), 1.94−2.25 (6H, m), 4.54 (1H, dd, *J* = 11.4, 3.0 Hz), 5.01 (2H, s), 5.52 (1H, s), 6.44 (1H, s), 6.92 (2H, d, *J* = 8.7 Hz), 7.24−7.43 (12H, m), 7.47 (1H, s). Anal. ($C_{33}H_{38}N_4O_2$) C, H, N.

*N-[1-(4-Chlorophenyl)-1-ethylpropyl]-7,7-dimethyl-5-phenyl-4,5,6,7-tetrahydropy-razolo[1,5-a]pyrimidine-3-carboxamide hydrochloride (**9a**).* To a solution of **8b** (350 mg, 0.78 mmol) in EtOAc (5 mL) was added 4 M HCl (0.5 mL, 2.0 mmol) in EtOAc at room temperature. Crystallization from EtOAc−hexane and the crystals was collected by filtration. Recrystallization from EtOAc−hexane afforded **9a** as HCl salt (270 mg, 71%), mp 160−162 °C. ^1H NMR ($CDCl_3$): δ 0.74 (3H, t, *J* = 7.2 Hz), 0.82 (3H, t, *J* = 7.2 Hz), 1.78 (3H, s), 1.94 (3H, s), 1.99−2.44 (6H, m), 4.56 (1H, t, *J* = 9.0 Hz), 7.23−7.38 (10H, m), 8.26 (1H, s), 9.86 (1H, s). Anal. ($C_{26}H_{32}Cl_2N_4O$) C, H, N.

*N-[1-(4-Chlorophenyl)-1-ethylpropyl]-7,7-dimethyl-5-phenyl-4,5,6,7-tetrahydropy-razolo[1,5-a]pyrimidine-3-carboxamide CH_3SO_3H salt (**9b**).* To a solution of **8b** (350 mg, 0.78 mmol) in EtOAc (5 mL) was added CH_3SO_3H (82 mg, 0.85 mmol) at room temperature. The solvent was concentrated in vacuo. Crystallization from EtOAc−hexane and recrystallization from EtOH−Et_2O afforded **9b** as CH_3SO_3H salt (390 mg, 92%), mp 147−149 °C. ^1H NMR ($CDCl_3$): δ 0.70−0.82 (6H, m), 1.71 (3H, s), 1.80 (3H, s), 1.88−2.34 (6H, m), 2.94 (3H, s), 4.56 (1H, dd, *J* = 9.6, 5.1 Hz), 7.13−7.36 (11H, m), 8.85 (1H, s). Anal. ($C_{27}H_{35}ClN_4O_4S\cdot0.5H_2O$) C, H, N.

*N-[1-(4-Chlorophenyl)-1-ethylpropyl]-7,7-dimethyl-5-phenyl-4,5,6,7-tetrahydropy-razolo[1,5-a]pyrimidine-3-carboxamide H_2SO_4 Salt (**9c**).* To a solution of **8b** (120 mg, 0.27 mmol) in Et_2O (2 mL) was added H_2SO_4 (29 mg, 0.30 mmol) at room temperature. The crystals was collected by filtration and washed with hexane to give **9c** as H_2SO_4 salt (110 mg, 75%), mp 137−139 °C. ^1H NMR ($CDCl_3$): δ 0.66−0.82 (6H, m), 1.69 (3H, s), 1.77 (3H, s), 1.92−2.04 (6H, m), 4.55−4.60 (1H, m), 7.20−7.37 (10H, m), 7.66 (1H, s), 8.42 (1H, brs), 9.91 (1H, s). Anal. ($C_{26}H_{33}ClN_4OS\cdot2.5H_2O$) C, H, N.

*N-[1-(4-Chlorophenyl)-1-ethylpropyl]-7,7-dimethyl-5-phenyl-4,5,6,7-tetrahydropy-razolo[1,5-a]pyrimidine-3-carboxamide CH_3CO_2H Salt (**9d**).* To a solution of **8b** (120 mg, 0.27 mmol) in EtOAc (5 mL) was added CH_3CO_2H (18 mg, 0.30 mmol) at room temperature. The mixture was concentrated in vacuo. Crystallization from Et_2O−hexane afforded **9d** as CH_3CO_2H salt (70 mg, 51%), mp 123−124 °C. ^1H NMR ($CDCl_3$): δ 0.71−0.83 (6H, m), 1.57 (3H, s), 1.64 (3H, s), 1.89−2.29 (6H, m), 2.10 (3H, s), 4.54 (1H, dd, *J* = 11.0, 3.4 Hz), 5.53 (1H, s), 6.41 (1H, s), 7.26−7.33 (9H, m), 7.52 (1H, s). Anal. ($C_{28}H_{35}ClN_4O_3$) C, H, N.

*N-[1-Ethyl-1-(4-methylphenyl)propyl]-7,7-dimethyl-5-phenyl-4,5,6,7-tetrahydrop-yrazolo[1,5-a]pyrimidine-3-carboxamide Hydrochloride (**9e**).* To a solution of **8g** (150 mg, 0.35 mmol) in Et_2O (3 mL) was added 4 M HCl in EtOAc (0.3 mL, 1.2 mmol) at room temperature. The crystals was collected by filtration, and recrystallization from EtOAc−hexane afforded **9e** as HCl salt (400 mg, 92%), mp 158−160 °C. ^1H NMR ($CDCl_3$): δ 0.70−0.86 (6H, m), 1.78 (3H, s), 1.94 (3H, s), 1.98−2.43 (6H, m), 4.55−4.60 (1H, t, *J* = 8.8 Hz), 7.08 (2H, d, *J* = 8.2 Hz), 7.28−7.35 (8H, m), 7.66 (1H, s), 8.12 (1H, s), 9.82 (1H, s). Anal. ($C_{27}H_{35}ClN_4O$) C, H, N.

*N-[1-Ethyl-1-(4-methylphenyl)propyl]-7,7-dimethyl-5-phenyl-4,5,6,7-tetrahydrop-yrazolo[1,5-a]pyrimidine-3-carboxamide CH_3SO_3H Salt (**9f**).* To a solution of **8g** (150 mg, 0.35 mmol) in EtOAc (3 mL) was added CH_3SO_3H (40 mg, 0.42 mmol) at room temperature. The mixture was concentrated in vacuo. Crystallization from EtOAc−hexane afforded **6f** as CH_3SO_3H salt (170 mg, 93%), mp 152−154 °C. ^{1}H NMR ($CDCl_3$): δ 0.69−0.83 (6H, m), 1.70 (3H, s), 1.79 (3H, s), 1.91−2.20 (6H, m), 2.29 (3H, s), 2.96 (3H, s), 4.53−4.60 (1H, m), 6.69 (1H, br s), 7.10 (2H, d, *J* = 8.2 Hz), 7.20−7.33 (8H, m), 8.69 (1H, br s). Anal. ($C_{28}H_{38}N_4O_4 \cdot 0.5H_2O$) C, H, N.

*Ethyl 4-(1-{[(7,7-Dimethyl-5-phenyl-4,5,6,7-tetrahydropyrazolo-[1,5-a]pyrimidine-3-yl)carbonyl]amino}-1-ethylpropyl)benzoate (**10**).* A mixture of **8i** (2.0 g, 3.69 mmol), dppf (0.1 g, 0.18 mmol), $Pd(OAc)_2$ (40 mg, 0.18 mmol), and Et_3N (0.82 g, 8.12 mmol) in EtOH (10 mL) was stirred at 80 °C under 1 atoms CO atmosphere for 3 days. The catalyst was removed by filtration, and the filtrate was concentrated in vacuo. The residue was diluted with EtOAc, washed with aqueous $NaHCO_3$ and brine, dried over $MgSO_4$, and concentrated in vacuo. The residue was chromatographed on SiO_2 with EtOAc−hexane (2:3) to give crystals **10** as prisms (1.55 g, 86%), mp 181−182 °C. ^{1}H NMR ($CDCl_3$): δ 0.72−0.84 (6H, m), 1.35 (3H, *J* = 6.8 Hz), 1.57 (3H, s), 1.64 (3H, s), 1.91−2.32 (6H, m), 4.34 (2H, q, *J* = 6.8 Hz), 4.54 (1H, dd, *J* = 11.0, 3.2 Hz), 5.57 (1H, s), 6.39 (1H, s), 7.26−7.35 (5H, m), 7.43 (2H, d, *J* = 8.4 Hz), 7.52 (1H, s), 7.99 (2H, d, *J* = 8.4 Hz). Anal. ($C_{29}H_{36}N_4O_3$) C, H, N.

*N-{1-Ethyl-1-[4-(hydroxymethyl)phenyl]propyl}-7,7-dimethyl-5-phenyl-4,5,6,7-tetrahydropyrazolo[1,5-a]pyrimidine-3-carboxamide (**11**).* To a solution of **10** (500 mg, 1.02 mmol) in THF (50 mL) was added LAH (117 mg, 3.0 mmol) at 0 °C. After stirred at the same temperature for 1 h, $Na_2SO_4 \cdot 10H_2O$ (0.96 g, 3 mmol) was added to the reaction mixture at 0 °C. The whole was stirred at room temperature for 30 min and then filtered through Celite. The solvent was concentrated in vacuo to give crystals. Recrystallization from EtOAc−hexane afforded **11** as prisms (0.38 g, 83%), mp 178−179 °C. ^{1}H NMR ($CDCl_3$): δ 0.72−0.83 (6H, m), 1.57 (3H, s), 1.64 (3H, s), 1.93−2.26 (6H, m), 4.54 (1H, dd, *J* = 11.4, 3.6 Hz), 4.66 (2H, s), 5.56 (1H, s), 6.43 (1H, s), 7.26−7.39 (9H, m), 7.50 (1H, s). Anal. ($C_{27}H_{34}N_4O_2$) C, H, N.

*4-(1-{[(7,7-Dimethyl-5-phenyl-4,5,6,7-tetrahydropyrazolo[1,5-a]pyrimidine-3-yl)carbonyl]amino}-1-ethylpropyl)benzyl Acetate (**12**).* To a mixture of **11** (200 mg, 0.45 mmol), Et_3N (91 mg, 0.90 mmol), and K_2CO_3 (75 mg, 0.54 mmol) in THF (10 mL) was added AcCl (42 mg, 0.54 mmol) at 0 °C. After being stirred at the room temperature overnight, the reaction mixture was poured into H_2O and extracted with EtOAc. The extract was washed with brine, dried over $MgSO_4$, and concentrated in vacuo. The residue was chromatographed on SiO_2 with EtOAc−hexane (1:1) to give **12** as crystals (0.10 g, 46%), mp 185−186 °C. ^{1}H NMR ($CDCl_3$): δ 0.72−0.83 (6H, m), 1.56 (3H, s), 1.64 (3H, s), 1.96−2.26 (6H, m), 2.08 (3H, s), 4.54 (1H, dd, *J* = 11.0, 3.2 Hz), 5.06 (2H, s), 5.54 (1H, s), 6.42 (1H, s), 7.25−7.38 (9H, m), 7.49 (1H, s). Anal. ($C_{29}H_{36}N_4O_3$) C, H, N.

*N-[1-Ethyl-1-(4-hydroxyphenyl)propyl]-7,7-dimethyl-5-phenyl-4,5,-6,7-tetrahydro-pyrazolo[1,5-a]pyrimidine-3-carboxamide (**13**).* A mixture of **8j** (0.15 g, 0.29 mmol) and 10%Pd−C (50 mg) in MeOH (20 mL) was stirred at room temperature under hydrogen atmosphere for 4 h. The catalyst was removed by filtration, and the filtrate was concentrated in vacuo to give crystals. Recrystallization from THF−hexane afforded **13** as prisms (0.12 g, 99%), mp 152−153 °C. ^{1}H NMR ($CDCl_3$): δ 0.72−0.81 (6H, m), 1.57 (3H, s), 1.64 (3H, s), 1.93−2.21 (6H, m), 4.56 (1H, dd, *J* = 11.4, 3.8 Hz), 5.54 (1H, s), 5.69 (1H, s), 6.45 (1H, s), 6.73 (2H, d, *J* = 8.4 Hz), 7.18−7.35 (7H, m), 7.50 (1H, s). Anal. ($C_{26}H_{32}N_4O_2$) C, H, N.

*4-(1-{[(7,7-Dimethyl-5-phenyl-4,5,6,7-tetrahydropyrazolo[1,5-a]-pyrimidine-3-yl)carbonyl]-amino}-1-ethylpropyl)phenyl Acetate (**14a**).* To a mixture of **13** (0.30 g, 0.69 mmol) and Et_3N (0.21 g, 2.08 mmol) in THF (20 mL) was added AcCl (60 mg, 0.76 mmol) at room temperature. After stirred at the same temperature for 1 h, the reaction mixture was poured into aqueous $NaHCO_3$, and extracted with EtOAc. The extract was washed with brine, dried over $MgSO_4$, and concentrated in vacuo. The residue was chromatographed on SiO_2 with EtOAc−hexane (1:1) to give crystals. Recrystallization from Et_2O−hexane afforded **14a** as prisms (0.28 g, 85%), mp 171−172 °C. ^{1}H NMR ($CDCl_3$): δ 0.72−0.83 (6H, m), 1.57 (3H, s), 1.64 (3H, s), 1.97−2.22 (6H, m), 2.27 (3H, s), 4.55 (1H, dd, *J* = 11.0, 3.4 Hz), 5.54 (1H, s), 6.43 (1H, s), 7.04 (2H, d, *J* = 8.8 Hz), 7.28−7.38 (7H, m), 7.49 (1H, s). Anal. ($C_{28}H_{34}N_4O_3 \cdot 0.1H_2O$) C, H, N.

*N-{1-Ethyl-1-[4-(2-oxobutoxy)phenyl]propyl}-7,7-dimethyl-5-phenyl-4,5,6,7-tetrahydropyrazolo[1,5-a]pyrimidine-3-carboxamide (**14b**).* A mixture of **13** (0.40 g, 0.92 mmol), K_2CO_3 (0.51 g, 3.68 mmol), and ethyl bromoacetate (0.18 g, 1.10 mmol) in DMF (10 mL) was stirred at room temperature for 2 h. The reaction mixture was poured into H_2O and extracted with EtOAc. The extract was washed with aqueous $NaHCO_3$ and brine, dried over $MgSO_4$, and concentrated in vacuo to give crystals. Recrystallization from EtOAc−hexane afforded **14b** as prisms (0.42 g, 88%), mp 178−179 °C. ^{1}H NMR ($CDCl_3$): δ 0.70−0.81 (6H, m), 1.29 (3H, t, *J* = 7.4 Hz), 1.56 (3H, s), 1.64 (3H, s), 1.94−2.22 (6H, m), 4.26 (2H, q, *J* = 7.4 Hz), 4.51−4.58 (1H, m), 4.58 (2H, s), 5.51 (1H, s), 6.43 (1H, s), 6.85 (2H, d, *J* = 8.8 Hz), 7.25−7.38 (7H, m), 7.48 (1H, s). Anal. ($C_{30}H_{38}N_4O_3$) C, H, N.

*Ethyl (5R)-7,7-Dimethyl-5-phenyl-4,5,6,7-tetrahydropyrazolo[1,5-a]pyrimidine-3-carboxylate (**15a**) and Ethyl (5S)-7,7-Dimethyl-5-phenyl-4,5,6,7-tetrahydropyrazolo[1,5-a]pyrimidine-3-carboxylate (**15b**).* Compound **6** (79.9 g, 0.27 mol) was separated by CHIRAL column HPLC (CHIRALCEL OD 50 mm I.D. × 500 mmL, hexane−EtOH/95:5, flow rate 60 mL/min, temperature 30 °C, detection (UV) 254 nm, 1shot approximately 800 mg, 100 times) to give **15a** (39.4 g, retention time 19.7 min: 99.8% ee) and **15b** (37.8 g, retention time 14.8 min: 99.8% ee). Analytical condition of **15a** and **15b** was CHIRAL column HPLC (CHIRALCEL OD 4.6 mm I.D. × 500 mmL, hexane: EtOH/95:5, flow rate 0.5 mL/min, temperature 30 °C, detection (UV) 254 nm, injection volume 10 μL). ^{1}H NMR ($CDCl_3$): δ 1.31 (3H, t, *J* = 7.0 Hz), 1.57 (3H, s), 1.64 (3H, s), 2.11−2.15 (2H, m), 4.23 (2H, q, *J* = 7.0 Hz), 4.64 (1H, dd, *J* = 9.4, 5.2 Hz), 6.03 (1H, s), 7.30−7.45 (5H, m), 7.64 (1H, s).

*(5R)-(+)-7,7-Dimethyl-5-phenyl-4,5,6,7-tetrahydropyrazolo[1,5-a]-pyrimidine-3-carboxylic acid (**16a**).* A mixture of **15a** (0.67 g, 2.24 mmol) and KOH (0.38 g, 6.77 mmol) in H_2O−EtOH (1:1, 40 mL) was stirred at 90 °C for 12 h and the solvent was concentrated in vacuo. The residue was diluted with EtOAc and acidified with 1N HCl. The organic layer was washed brine, dried over $MgSO_4$, and concentrated in vacuo to give **16a** as crystals (0.55 g, 82%), mp 205−206 °C; $[\alpha]_D^{20}$ = 86.01 (*c* 0.48, $CHCl_3$). ^{1}H NMR ($CDCl_3$): δ 1.59 (3H, s), 1.66 (3H, s), 2.05−2.15 (2H, m), 4.64 (1H, dd, *J* = 9.6, 5.4 Hz), 6.04 (1H, s), 7.30−7.41 (5H, m), 7.73 (1H, s).

*(5S)-(−)-7,7-Dimethyl-5-phenyl-4,5,6,7-tetrahydropyrazolo[1,5-a]-pyrimidine-3-carboxylic Acid (**16b**).* A mixture of **15b** (0.73 g, 2.44 mmol) and KOH (0.41 g, 7.32 mmol) in H_2O−EtOH (1:1, 40 mL) was stirred at 90 °C for 12 h, and the solvent was concentrated in vacuo. The residue was diluted with EtOAc and acidified with 1N HCl. The organic layer was washed brine, dried over $MgSO_4$, and concentrated in vacuo to give **16b** as crystals (0.55 g, 83%), mp 205−206 °C; $[\alpha]_D^{20}$ = −85.33 (*c* 0.46, $CHCl_3$). ^{1}H NMR ($CDCl_3$): δ 1.59 (3H, s), 1.66 (3H, s), 2.05−2.15 (2H, m), 4.64 (1H, dd, *J* = 9.6, 5.4 Hz), 6.04 (1H, s), 7.30−7.41 (5H, m), 7.73 (1H, s).

*(5R)-(−)-N-[1-Ethyl-1-(4-methylphenyl)propyl]-7,7-dimethyl-5-phenyl-4,5,6,7-tetrahydropyrazolo[1,5-a]pyrimidine-3-carboxamide Hydrochloride (**17a**).* To a mixture of **16a** (25.0 g, 92.1 mmol) and DMF (1.5 mL) in toluene (250 mL) was added $SOCl_2$ (13.75 mL, 189 mmol) at room temperature. After stirring at the same temperature for 1 h, the solvent was evaporated off. A mixture of 3-(4-methylphenyl)pentan-3-amine

hydrochloride (23.65 g, 111 mmol) and Et_3N (28.0 g, 277 mmol) in toluene (250 mL) was stirred at 70 °C for 1 h, and then acid chloride obtained in toluene was added to the reaction mixture at 70 °C. After stirring at the same temperature for 3 h, the reaction mixture was poured into H_2O and extracted with EtOAc. The extract was washed with brine, dried over $MgSO_4$, and concentrated in vacuo. The residue was chromatographed on SiO_2 with EtOAc−hexane (1:1) to give crystals. To a solution of the crystals obtained in Et_2O (150 mL) was added 4N HCl in EtOAc (25.0 mL, 100 mmol) at 0 °C. The crystals were collected by filtration and washed with Et_2O (35.5 g, 83%), mp 142−143 °C; $[\alpha]_D^{21}$ = −27.99 (*c* 0.80, $CHCl_3$). ^1H NMR ($CDCl_3$): δ 0.69−0.86 (6H, m), 1.78 (3H, s), 1.94 (3H, s), 1.98−2.46 (6H, m), 4.54 (1H, t, *J* = 8.8 Hz), 7.08 (2H, d, *J* = 8.2 Hz), 7.29−7.35 (8H, m), 8.15 (1H, s), 9.83 (1H, s). Anal. ($C_{27}H_{35}ClN_4O \cdot 0.25H_2O$) C, H, N.

*(5S)-(+)-N-[1-Ethyl-1-(4-methylphenyl)propyl]-7,7-dimethyl-5-phenyl-4,5,6,7-tetrahydropyrazolo[1,5-a]pyrimidine-3-carboxamide Hydrochloride (**17b**).* To a mixture of **16b** (0.10 g, 0.37 mmol) and DMF (1 drop) in toluene (1 mL) was added $SOCl_2$ (0.05 mL, 0.69 mmol) at room temperature. After stirring at the same temperature for 1 h, the solvent was evaporated off. A mixture of 3-(4-methylphenyl)-pentan-3-amine hydrochloride (95 mg, 0.44 mmol) and Et_3N (0.11 g, 1.11 mmol) in toluene (1 mL) was stirred at 70 °C for 1 h, and then acid chloride obtained in toluene was added to the reaction mixture at 70 °C. After stirring at the same temperature for 3 h, the reaction mixture was poured into H_2O and extracted with EtOAc. The extract was washed with brine, dried over $MgSO_4$, and concentrated in vacuo. The residue was chromatographed on SiO_2 with EtOAc−hexane (1:1) to give crystals. To a solution of the crystals obtained in Et_2O was added 4N HCl in EtOAc (0.2 mL, 0.80 mmol) at 0 °C. The crystals were collected by filtration and washed with Et_2O (0.08 g, 47%), mp 142−143 °C; $[\alpha]_D^{21}$ = 31.05 (*c* 0.65, $CHCl_3$). ^1H NMR ($CDCl_3$): δ 0.76−0.85 (6H, m), 1.78 (3H, s), 1.94 (3H, s), 1.98−2.44 (6H, m), 4.55−4.60 (1H, dd, *J* = 9.6, 5.4 Hz), 7.09 (2H, d, *J* = 7.8 Hz), 7.28−7.34 (8H, m), 8.04 (1H, s), 9.76 (1H, s). Anal. ($C_{27}H_{35}ClN_4O \cdot 0.25H_2O$) C, H, N.

*(5S)-N-{1-Ethyl-1-[4-(trifluoromethyl)phenyl]propyl}-7,7-dimethyl-5-phenyl-4,5,6-,7-tetrahydropyrazolo[1,5-a]pyrimidine-3-carboxamide (**17c**).* To a mixture of **16b** (100 mg, 0.37 mmol) and DMF (1 drop) in toluene (2 mL) was added $SOCl_2$ (66 mg, 0.91 mmol) at room temperature. After stirring at the same temperature for 1 h, the solvent was evaporated off. A mixture of 3-(4-trifluoromethylphenyl)pentan-3-amine hydrochloride (129 mg, 0.61 mmol) and Et_3N (75 mg, 0.74 mmol) in toluene (2 mL) was stirred at 70 °C for 1 h, and then the acid chloride obtained in toluene was added to the reaction mixture at 70 °C. After stirring at the same temperature for 1 h, the reaction mixture was poured into H_2O and extracted with EtOAc. The extract was washed with H_2O and brine, dried over $MgSO_4$, and concentrated in vacuo to give crystals. Recrystallization from *i*PrOH afforded **17c** (85 mg, 47%), mp 163−164 °C. ^1H NMR ($CDCl_3$): δ 0.71−0.84 (6H, m), 1.21 (6H, d, *J* = 6.3 Hz), 1.57 (3H, s), 1.64 (3H, s), 1.90−2.31 (6H, m), 4.00−4.04 (1H, m), 4.54 (1H, dd, *J* = 11.4, 3.0 Hz), 5.56 (1H, s), 6.38 (1H, s), 7.26−7.58 (9H, m). Anal. ($C_{27}H_{31}F_3N_4O \cdot 1.0i\text{-PrOH}$) C, H, N.

Biological Method. *GTPγS Binding Assay.* The GTPγS binding activity was measured as follows. The CaR-expressing cell membrane was incubated with test compounds for 10 min. The assays were carried out at room temperature for an hour in a reaction solution mixture containing 20 mM HEPES (pH.7.4), 100 mM NaCl, 1 mM $MgCl_2$, 167 μg/mL DTT, 5 μM guanosine 5′-diphosphate, 0.4 nM [35S]-guanosine 5′-(γ-thio) triphosphate ([35S]-GTPγS), and 6 mM $CaCl_2$. The mixture was filtered through a GF/C filter. After washing the fourth time with 300 μL of phosphate-buffered saline, radioactivity of the filter was measured using a Top-Count scintillation counter. Data from GTPγS binding assays for antagonists were analyzed with the use of the Prism program (GraphPad Software, Inc.). IC_{50} values were determined through nonlinear regression analysis performed with Prism.

Measurement of in Vivo PTH Secretion. To estimate in vivo PTH secretion of these compounds in rat, plasma intact PTH levels were assayed using a rat enzyme-linked immunosorbent assay (ELISA) kit (Rat Bioactive Intact PTH ELISA kit, Immutopics, Inc.) after oral administration.

Bone-Forming Test in OVX Rat Models. Three-month-old virgin Crj:CD(SD)IGS rats were subjected either to a bilateral ovariectomy or to a sham surgery under anesthesia. The OVX rats were divided into two groups that were matched by the body weight. Sham rats and one group of OVX rats received an oral dose of a vehicle (0.5% aqueous solution of methylcellulose). The remaining OVX groups orally received **9e** (10 mg/kg) suspended in the vehicle. From the next day of the operation, the oral treatment continued daily for 3 months. Two months after starting treatment, a blood sample was collected for osteocalcin measurement. The plasma was obtained by centrifugation, and the supernatants were collected and plasma osteocalcin levels were measured by RIA (Immupopics, San Clemente, CA). One day after the last treatment, animals were sacrificed and the right femur and tibia were removed for the bone mineral density (BMD) evaluation. The BMD of the distal femur and proximal tibia were quantified by X-ray-CT scanner for small animals (LaTheta LCT-100A, ALOKA, Japan).

Metabolic Stability Assay. Metabolic stability assay hepatic microsomes from mice, rats, and humans were purchased from Xenotech, LLC (Lenexa, KS). An incubation mixture with a final volume of 0.1 mL consisted of microsomal protein in 50 mmol/L KH_2PO_4−K_2HPO_4 phosphate buffer (pH 7.4) and 1 mmol/L test compound. The concentration of hepatic microsomal protein was 0.2 mg/mL. An NADPH-generating system containing 50 mmol/L $MgCl_2$, 50 mmol/L glucose-6-phosphate, 5 mmol/L β-NADP+, and 15 unit/mL glucose-6-phosphate dehydrogenase was prepared and added to the incubation mixture with a 10% volume of the reaction mixture. After the addition of the NADPH-generating system, the mixture was incubated at 37 °C for 0 and 20 min. The reaction was terminated by the addition of acetonitrile equivalent to the volume of the reaction mixture. All incubations were made in duplicate. Test compound in the reaction mixture was measured by HPLC system equipped with a UV detector. For metabolic stability determinations, chromatograms were analyzed for parent compound disappearance from the reaction mixtures.

Measurement of Solubility. The compounds were added to the aqueous buffer solution (pH6.8 + bile acid: 20 mmol/L sodium glycochenodeoxycholate). After incubation, precipitates were separated by filtration. The thermodynamic solubility was determined by HPLC analysis of each filtrate.

Plasma Concentration in Rats. Compound **9e** was administered orally to nonfasted Crl:CD(SD) rats (female, 12 weeks old, *n* = 3) at a dose of 10 mg/kg in 0.5% methylcellulose suspension. At 0.25, 0.5, 1, 2, 4, 8, and 24 h after oral administration, blood samples were collected and immediately centrifuged to obtain the plasma fraction. The plasma samples were deproteinized with acetonitrile. After centrifugation, the supernatant obtained was diluted with 0.01 mol/L ammonium acetate and centrifuged again. The compound concentration in the supernatant was measured by high performance LC system (SHIMADZU, Kyoto, Japan) consisting of a binary solvent manager (LC-10AD_{vp}), sample organizer (SCL-10AD_{vp}), sample manager (SIL-10A_{vp}), and column oven (CTO-10AC). The HPLC conditions were as follows: column, L-column ODS (4.6 mm × 250 mm) from Chemicals Evaluation and Research Institute (Tokyo, Japan); mobile phase, (A) 0.01 mol/L ammonium acetate/(B) acetonitrile = 3/7; flow rate, 1.0 mL/min; column temperature, 40 °C; wavelength, 262 nm.

Permeability of Test Compounds across Caco-2 Monolayers. Caco-2 monolayers were grown to confluence on collagen-coated, microporous, polycarbonate membranes in 12-well Costar Transwell plates. The permeability assay buffer was Hanks' Balanced Salt Solution containing 10 mmol/L HEPES, 15 mmol/L glucose, and 1% bovine serum albumin

at a pH of 7.3−7.5. The test compound dosing concentrations were 10 μmol/L in the assay buffer. The cells were dosed on the apical side (A-to-B) or basolateral side (B-to-A) and incubated at 37 °C with 5% CO_2 in a humidified chamber. At each time point, 1 and 2 h, 200 μL were taken from the A-to-B receivers, and 50 μL were taken from the B-to-A receivers. Fresh assay buffer was added to the receivers after the 1 h sampling. Also, at 2 h, 50 μL of the donors were taken. Each determination was performed in duplicate. The permeability through a cell-free (blank) membrane was studied to determine nonspecific binding and free diffusion of the test compounds through the device. The lucifer yellow flux was also measured for each monolayer after being subjected to the test compounds to ensure no damage was inflicted to the cell monolayers during the flux period. All samples were assayed by LC/MS/MS using electrospray ionization. The apparent permeability, P_{app}, and percent recovery were calculated as follows: $P_{app} = (dC_r/dt) \times V_r/(A \times C_0)$ (eq 1). Percent recovery = $100((V_r \times C_r^{final}) + (V_d \times C_d^{final}))/(V_d \times C_0)$ (eq 2). Where, dC_r/dt is the slope of the cumulative concentration in the receiver compartment versus time in μmol/L s^{-1}. V_r is the volume of the receiver compartment in cm^3. V_d is the volume of the donor compartment in cm^3. A is the area of the cell monolayer (1.1 cm^2 for 12-well Transwell). C_0 is the nominal concentration of the dosing solution in μmol/L. C_r^{final} is the cumulative receiver concentration in μmol/L at the end of the incubation period. C_d^{final} is the concentration of the donor in μmol/L at the end of the incubation period.

■ ASSOCIATED CONTENT

Ⓢ Supporting Information. Methods and instrumentation used to obtain the X-ray crystal structure of compound **17c**; elemental analyses data for compounds **3**, **8**−**14**, and **17**. This material is available free of charge via the Internet at http://pubs.acs.org.

Accession Codes

†CCDC codes: CCDC 800340.

■ AUTHOR INFORMATION

Corresponding Author

*Phone: +81-6-6308-9081. Fax: +81-6-6300-6306. E-mail: Yoshida_Masato@takeda.co.jp.

■ ACKNOWLEDGMENT

We thank Dr. S. Ohkawa and the late Dr. M. Kawase for their encouragement and helpful advice. We thank K. Higashikawa for X-ray crystallographic analysis, and Dr. T. Yamano and S. Yamamoto for optical resolution, Dr. M. Yamaguchi for obtaining rat pharmacokinetic study, and Dr. T. Okuda for measurement of metabolic stability. We thank N. Tsuruta for in vivo assays.

■ ABBREVIATIONS USED

CaSR, calcium sensing receptor; PTH, parathyroid hormone; OVX rat, osteopenic ovariectomized rat; GPCR, G-protein coupled receptor; HTOS, high throughput organic synthesis; HATU, 2-(1*H*-7-azabenzotriazole-1-yl)-1,1,3,3-tetramethyl uronium hexafluorophosphate; BMD, bone mineral density

■ REFERENCES

(1) Ettinger, M. P. Aging bone and osteoporosis: strategies for preventing fractures in the elderly. *Arch. Intern. Med.* **2003**, *163*, 2237–2246.

(2) Tarantino, U.; Cannata, G.; Lecce, D.; Celi, M.; Cerocchi, I.; Iundusi, R. Incidence of fragility fractures aging. *Aging Clin. Exp. Res.* **2007**, *19*, 7–11.

(3) Cummings, S. R.; Melton, L. J. Epidemiology and outcomes of osteoporotic fractures. *Lancet* **2002**, *359*, 1761–1767.

(4) Black, D. M.; Cummings, S. R.; Karpf, D. B.; Cauley, J. A.; Thompson, D. E.; Nevitt, M. C.; Bauer, D. C.; Genant, H. K.; Haskell, W. L.; Marcus, R.; Ott, S. M.; Torner, J. C.; Quandt, S. A.; Reiss, T. F.; Ensrud, K. E.; Fracture Intervention Trial Research Group. Randomised trial of effect of alendronate on risk of fracture in women with existing vertebral fractures. *Lancet* **1996**, *348*, 1535–1541.

(5) Reginster, J.; Minne, H. W.; Sorensen, O. H.; Hooper, M.; Roux, C.; Brandi, M. L.; Lund, B.; Ethgen, D.; Pack, S.; Roumagnac, I.; Eastell, R.; On behalf of the Vertebral Efficacy with Risedronate Therapy (VERT) Study Group. Randomized trial of the effects of risedronate on vertebral fractures in women with established postmenopausal osteoporosis. *Osteoporosis Int.* **2000**, *11*, 83–91.

(6) Ettinger, B.; Black, D. M.; Mitlak, B. H.; Knickerbocker, R. K.; Nickelsen, T.; Genant, H. K.; Christiansen, C.; Delmas, P. D.; Zanchetta, J. R.; Stakkestad, J.; Glüer, C. C.; Krueger, K.; Cohen, F. J.; Eckert, S.; Ensrud, K. E.; Avioli, L. V.; Lips, P.; Cummings, S. R.; Multiple Outcomes of Raloxifene Evaluation (MORE) Investigators. Reduction of vertebral fracture risk in postmenopausal women with osteoporosis treated with raloxifene: results from a 3-year randomized clinical trial. *JAMA, J. Am. Med. Assoc.* **1999**, *282*, 637–645.

(7) Pleiner-Duxneuner, J.; Zwettler, E.; Paschalis, E.; Roschger, P.; Nell-Duxneuner, V.; Klaushofer, K. Treatment of osteoporosis with parathyroid hormone and teriparatide. *Calcif. Tissue Int.* **2009**, *84*, 159–170.

(8) Dobnig, H. A review of teriparatide and its clinical efficacy in the treatment of osteoporosis. *Expert Opin. Pharmacother.* **2004**, *5*, 1153–1162.

(9) Neer, R. M.; Arnaud, C. D.; Zanchetta, J. R.; Prince, R.; Gaich, G. A.; Reginster, J. Y.; Hodsman, A. B.; Eriksen, E. F.; Ish-Shalom, S.; Genant, H. K.; Wang, O.; Mitlak, B. H. Effect of parathyroid hormone (1−34) on fractures and bone mineral density in postmenopausal women with osteoporosis. *N. Engl. J. Med.* **2001**, *344*, 1434–1441.

(10) Lotinun, S.; Sibonga, J. D.; Turner, R. T. Differential effects of intermittent and continuous administration of parathyroid hormone on bone histomorphometry and gene expression. *Endocrine* **2002**, *17*, 29–36.

(11) Frolik, C. A.; Black, E. C.; Cain, R. L.; Satterwhite, J. H.; Brown-Augsburger, P. L.; Sato, M.; Hock, J. M. Anabolic and catabolic bone effects of human parathyroid hormone (1−34) are predicted by duration of hormone exposure. *Bone* **2003**, *33*, 372–379.

(12) Gerspacher, M; Altmann, E; Beerli, R; Buhl, T; Endres, R; Gamse, R; Kameni-Tcheudji, J; Kneissel, M; Krawinkler, K. H.; Missbach, M; Schmidt, A; Seuwen, K; Weiler, S; Widler, L. Penta-substituted benzimidazoles as potent antagonists of the calcium-sensing receptor (CaSR-antagonists). *Bioorg. Med. Chem. Lett.* **2010**, *17*, 5161–5164.

(13) Chattopadhyay, N. Biochemistry, physiology and pathophysiology of the extracellular calcium-sensing receptor. *Int. J. Biochem. Cell Biol.* **2000**, *32*, 789–804.

(14) Fox, J.; Miller, M. A.; Stroup, G. B.; Nemeth, E. F.; Miller, S. C. Plasma levels of parathyroid hormone that induce anabolic effects in bone of ovariectomized rats can be achieved by stimulation of endogenous hormone secretion. *Bone* **1997**, *21*, 163–169.

(15) Gowen, M.; Stroup, G. B.; Dodd, R. A.; James, I. E.; Votta, B. J.; Smith, B. R.; Bhatnagar, P. K.; Lago, A. M.; Callahan, J. F.; DelMar, E. G.; Miller, M. A.; Nemeth, E. F.; Fox, J. Antagonizing the parathyroid calcium receptor stimulates parathyroid hormone secretion and bone formation in osteopenic rats. *J. Clin. Invest.* **2000**, *105*, 1595–1604.

(16) Kumar, S.; Matheny, C. J.; Hoffman, S. J.; Marquis, R. W.; Schultz, M.; Liang, X.; Vasko, J. A.; Stroup, G. B.; Vaden, V. R.; Haley, H.; Fox, J.; Delmar, E. G.; Nemeth, E. F.; Lago, A. M.; Callahan, J. F.; Bhatnagar, P.; Huffman, W. F.; Gowen, M.; Yi, B.; Danoff, T. M.; Fitzpatrick, L. A. An orally active calcium-sensing receptor antagonist

that transiently increases plasma concentrations of PTH and stimulates bone formation. *Bone* **2010**, *46*, 534–542.

(17) Carter, P. H.; Liu, R. Q.; Foster, W. R.; Tamasi, J. A.; Tebben, A. J.; Favata, M.; Staal, A.; Cvijic, M. E.; French, M. H.; Dell, V.; Apanovitch, D.; Lei, M.; Zhao, Q.; Cunningham, M.; Decicco, C. P.; Trzaskos, J. M.; Feyen, J. H. Discovery of a small molecule antagonist of the parathyroid hormone receptor by using an N-terminal parathyroid hormone peptide probe. *Proc. Natl. Acad. Sci. U.S.A.* **2007**, *104*, 6846–6851.

(18) Yoshida, M.; Mori, A.; Inaba, A.; Oka, M.; Makino, H.; Yamaguchi, M.; Fujita, H; Kawamoto, T.; Goto, M.; Kimura, H.; Baba, A.; Yasuma, T. Synthesis and structure−activity relationship of tetrahydropyrazolopyrimidine derivatives—a novel structural class of potent calcium-sensing receptor antagonists. *Bioorg. Med. Chem.* **2010**, *18*, 8501–8511.

(19) X-ray crystallographic data for compound **17c** has been deposited with the Cambridge Crystallographic Data Center as CCDC 800340. The crystallographic data can be obtained, free of charge, on application to CCDC, 12 Union Road, Cambridge CB2 1EZ, UK (fax: +44-(0)1223−336033 or e-mail: deposit@ccdc.cam.ac.uk).

(20) Fox, J.; Miller, M. A.; Newman, M. K.; Metcalfe, A. F.; Turner, C. H.; Recker, R. R.; Smith, S. Y. Daily treatment of aged ovariectomized rats with human parathyroid hormone (1−84) for 12 months reverses bone loss and enhances trabecular and cortical bone strength. *Calcif. Tissue Int.* **2006**, *79*, 262–272.